

# Supporting Information

## **Theoretical investigations of the substituent effect on the electronic and charge transport properties of the butterfly molecules**

Lijuan Wang, Jianhong Dai\* and Yan Song\*

School of Materials Science and Engineering, Harbin Institute of Technology at Weihai,  
2West Wenhua Road, Weihai, 264209, China.

\*E-mail: sy@hitwh.edu.cn; daijh@hit.edu.cn.

## Contents

**Figure S1.** Optimized geometries of molecules 1 to 6.

**Figure S2.** Chemical structures of molecules 1 to 6, with atom indices labeled on the structures.

**Figure S3.** Contributions of the vibrational modes to the relaxation energies for molecules 1, 3 and 5, embedded with the normal modes contribute the most for the reorganization energies of holes.

**Figure S4.** Contributions of the vibrational modes to the relaxation energies for molecules 1 and 5, embedded with the normal modes contribute the most for the reorganization energies of electrons.

**Figure S5.** The pictorial HOMO-HOMO (a), and LUMO-LUMO (b) interactions of the most prominent pathway in molecule 1 from side view and top view.

**Figure S6.** The pictorial HOMO-HOMO (a), and LUMO-LUMO (b) interactions of the most prominent pathway in molecule 2 from side view and top view.

**Figure S7.** The pictorial HOMO-HOMO (a), and LUMO-LUMO (b) interactions of the most prominent pathway in molecule 3 from side view and top view.

**Figure S8.** The pictorial HOMO-HOMO (a), and LUMO-LUMO (b) interactions of the most prominent pathway in molecule 5 from side view and top view.

**Figure S9.** The crystal packing and short contact interactions of the dominated charge hopping routes in molecules 1 to 6.

**Figure S10.** The projecting angle-dependent hopping paths to a transistor channel in the *ab* plane (a) and the calculated angle-resolved anisotropic hole (b) and electron (c) mobilities of molecule 1.

**Figure S11.** The projecting angle-dependent hopping paths to a transistor channel in the *ab* plane (a) and the calculated angle-resolved anisotropic hole (b) and electron (c) mobilities of molecule 2.

**Figure S12.** The projecting angle-dependent hopping paths to a transistor channel in the *ab* plane (a) and the calculated angle-resolved anisotropic hole (b) and electron (c) mobilities of molecule 3.

**Figure S13.** The projecting angle-dependent hopping paths to a transistor channel in the *ab* plane (a) and the calculated angle-resolved anisotropic hole (b) and electron (c) mobilities of molecule 5.

**Figure S14.** Plots of the reduced density gradient versus the electron density multiplied by the sign of the second Hessian eigenvalue. The data are obtained at B3LYP-D3/6-311G\* level.

**Figure S15.** Gradient isosurfaces for (a) dimer 1 of molecule 3, (b) dimer 1 of molecule 4, and (c) dimer 1 of molecule 6. The surfaces are colored on a blue-green-red scale according to values of  $\text{sign}(\lambda_2)\rho$ , ranging from -0.04 to 0.02 au. Blue indicates strong attractive interactions,

green indicates Van der Waals interactions and red indicates strong repulsion.

**Table S1.** The selected optimized bond lengths, bond angle and dihedral angles of molecules 1 to 3 in the neutral and ionic states, together with experimental values (the unit of bond lengths is in angstroms, and the bond angles and dihedral angles are in degrees).

**Table S2.** The selected optimized bond lengths, bond angle and dihedral angles of molecules 4 to 6 in the neutral and ionic states, together with experimental values (the unit of bond lengths is in angstroms, and the bond angles and dihedral angles are in degrees).

**Table S3.** The transfer integrals of hole ( $V_{\text{hole}}$ ) and electron ( $V_{\text{electron}}$ ) (absolute value) for different hopping pathways of molecules 1 to 6 based on B3LYP/6-31G(d, p) level.

**Table S4.** The calculated average mobilities of hole ( $\mu_{\text{h,ave.}}$ ) and electron ( $\mu_{\text{e,ave.}}$ ) of molecules 1 to 6 based on B3LYP/6-31G (d, p) level.

**Table S5** Intermolecular interaction energies for the most prominent dimers of molecules 3, 4 and 6.

**Table S6.** The reorganization energies of hole ( $\lambda^+$ ) and electron ( $\lambda^-$ ) using adiabatic potential energy surfaces (APES) approach, the HOMO, LUMO energies, as well as the vertical and adiabatic ionization potentials ( $IP_V$ ,  $IP_A$ ) and electron affinities ( $EA_V$ ,  $EA_A$ ) of molecule 6 at B3LYP-D3/6-31G (d, p) level: All the data are in unit of eV.

**Table S7** The transfer integrals of hole ( $V_{\text{hole}}$ ) and electron ( $V_{\text{electron}}$ ) (absolute value) for different hopping pathways and charge mobilities of hole and electron for molecule 6 based on B3LYP-D3/6-31G(d, p) level.

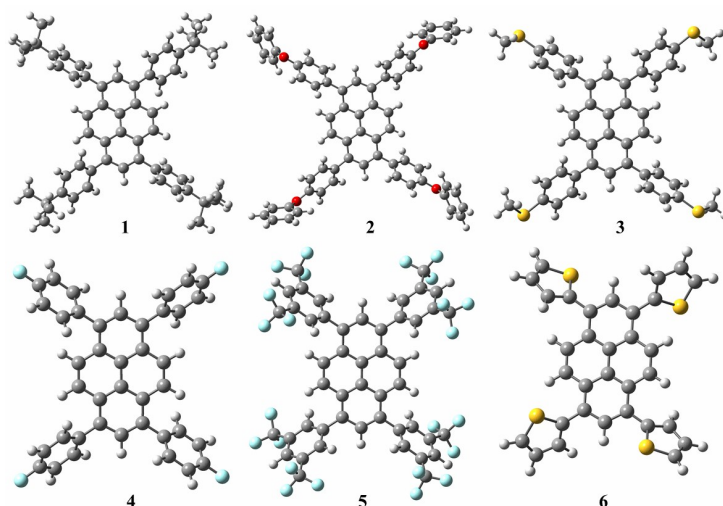


**Figure S1.** Optimized geometries of molecules 1 to 6.

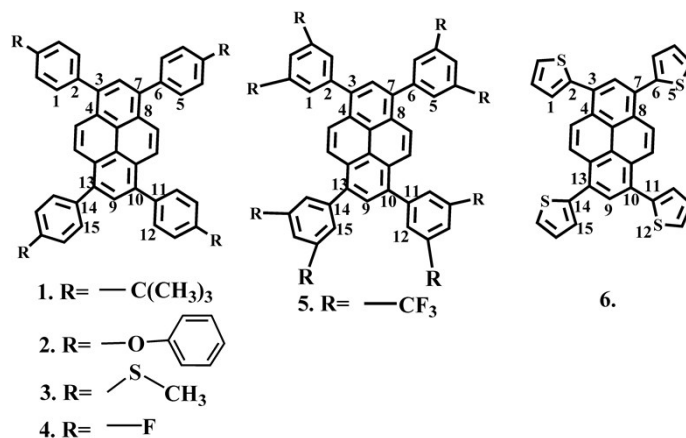


**Figure S2.** Chemical structures of molecules 1 to 6, with atom indices labeled on the structures.

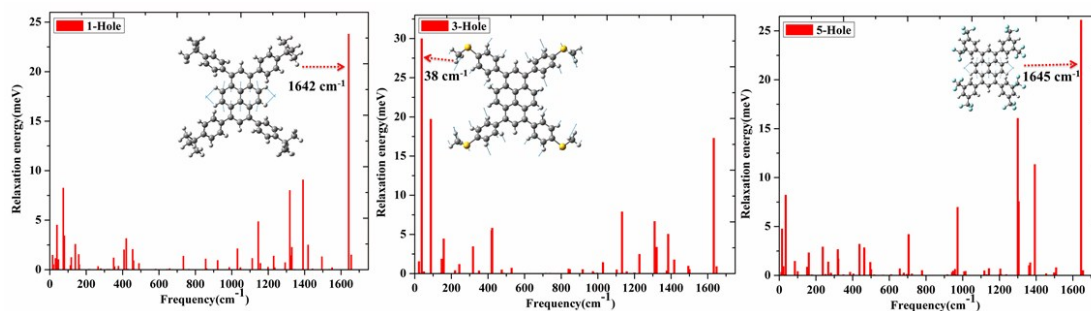


**Figure S3.** Contributions of the vibrational modes to the relaxation energies for molecules 1, 3 and 5, embedded with the normal modes contribute the most for the reorganization energies of holes.

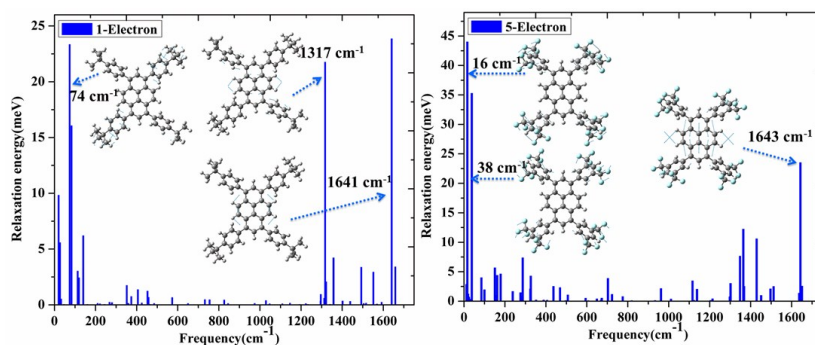


**Figure S4.** Contributions of the vibrational modes to the relaxation energies for molecules 1 and 5, embedded with the normal modes contribute the most for the reorganization energies of electrons.

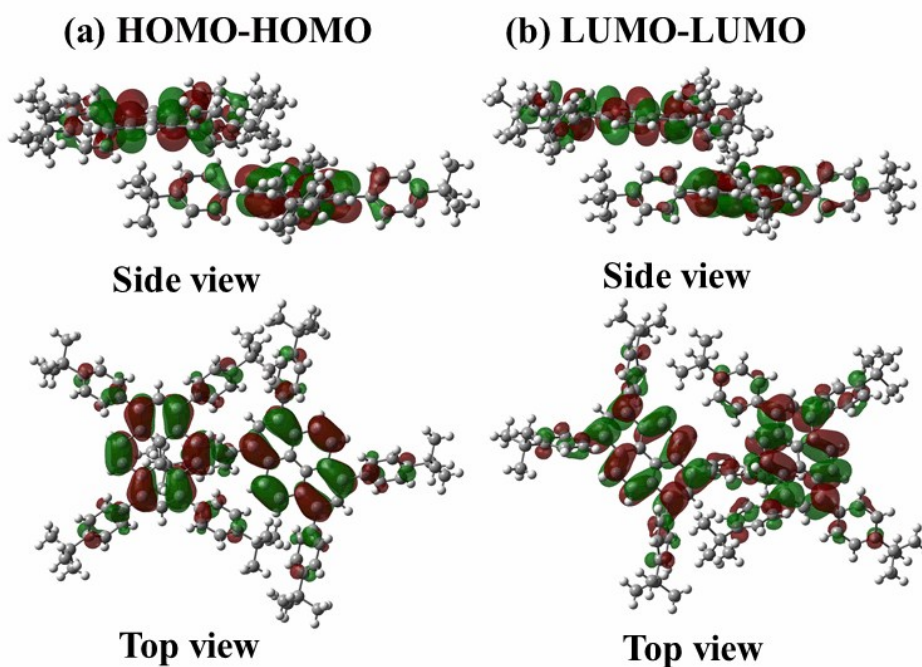


**Figure S5.** The pictorial HOMO-HOMO (a), and LUMO-LUMO (b) interactions of the most prominent pathway in molecule 1 from side view and top view.

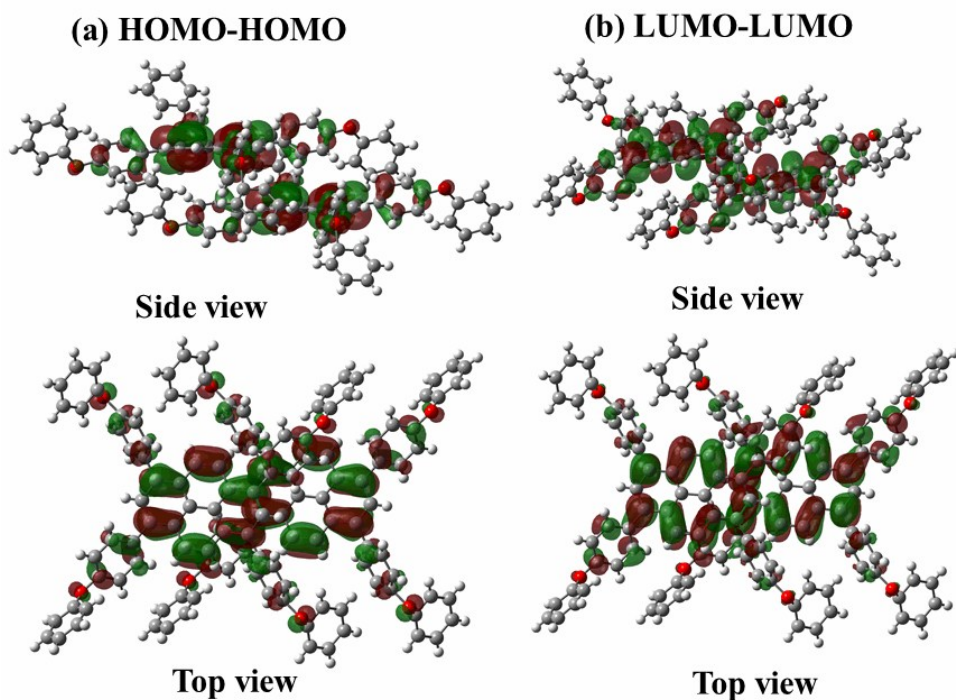


**Figure S6.** The pictorial HOMO-HOMO (a), and LUMO-LUMO (b) interactions of the most prominent pathway in molecule 2 from side view and top view.

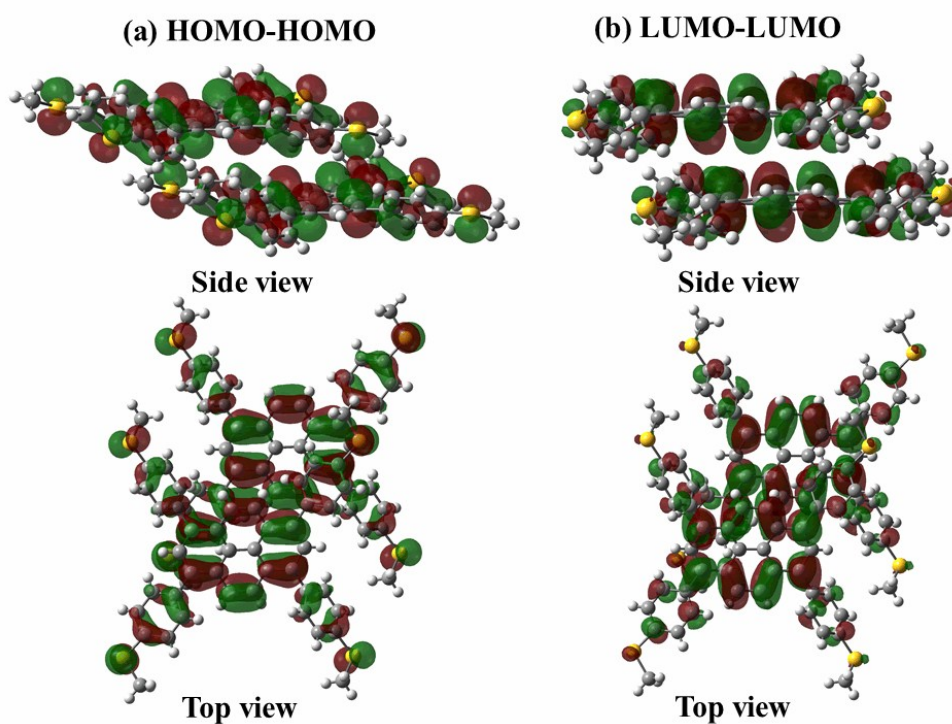


**Figure S7.** The pictorial HOMO-HOMO (a), and LUMO-LUMO (b) interactions of the most prominent pathway in molecule 3 from side view and top view.



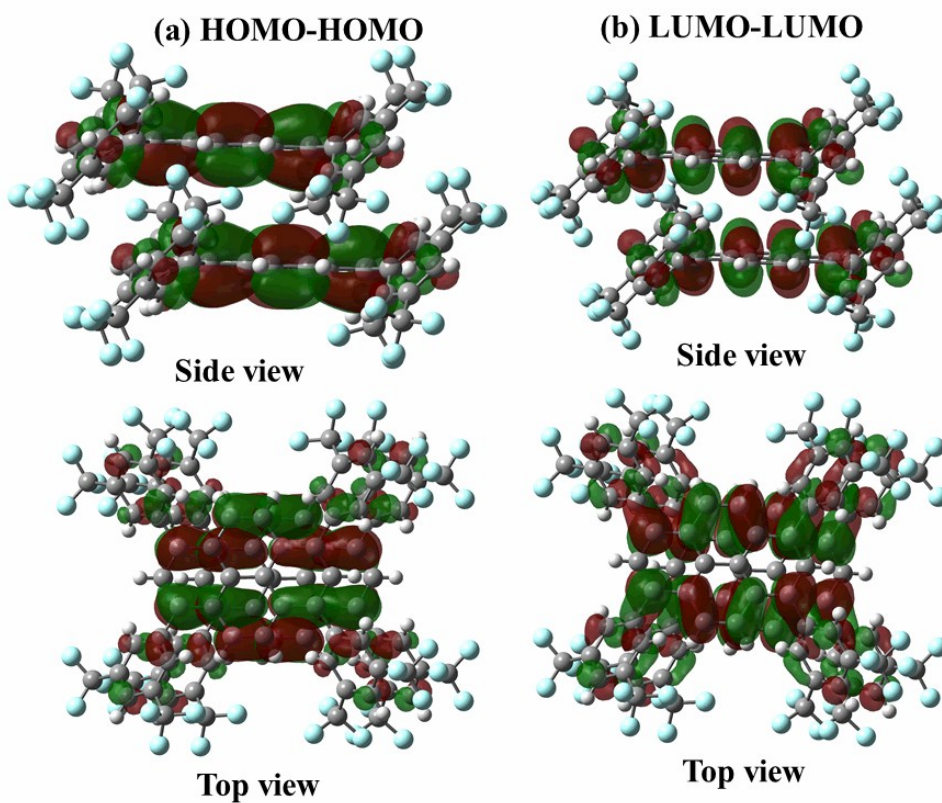


**Figure S8.** The pictorial HOMO-HOMO (a), and LUMO-LUMO (b) interactions of the most prominent pathway in molecule 5 from side view and top view.

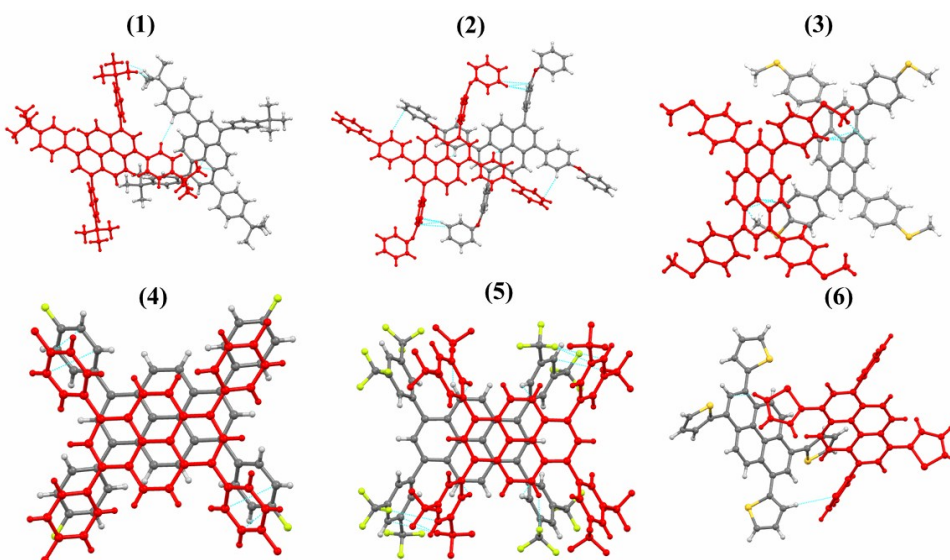


**Figure S9.** The crystal packing and short contact interactions of the dominated charge hopping routes in molecules 1 to 6.

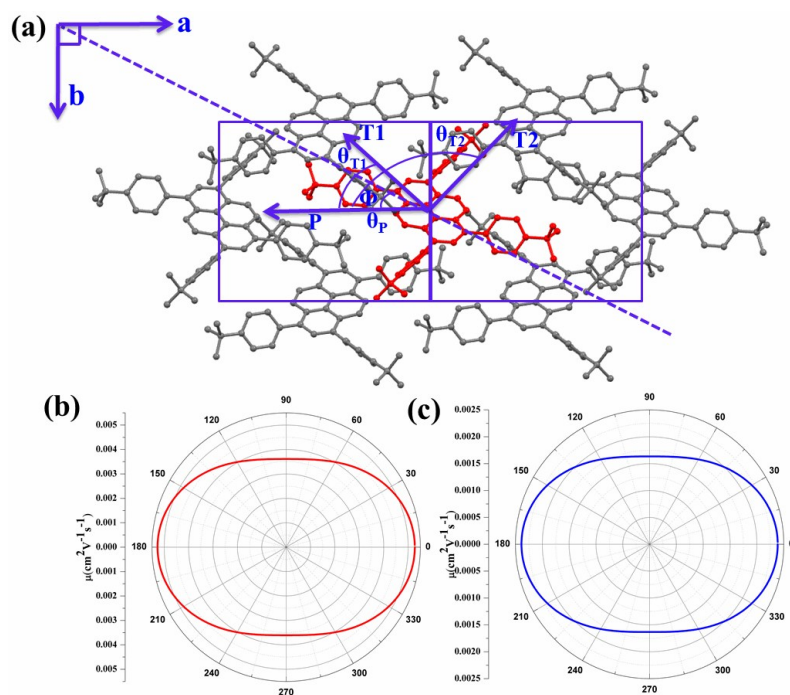


**Figure S10.** The projecting angle-dependent hopping paths to a transistor channel in the  $ab$  plane (a) and the calculated angle-resolved anisotropic hole (b) and electron (c) mobilities of molecule 1.

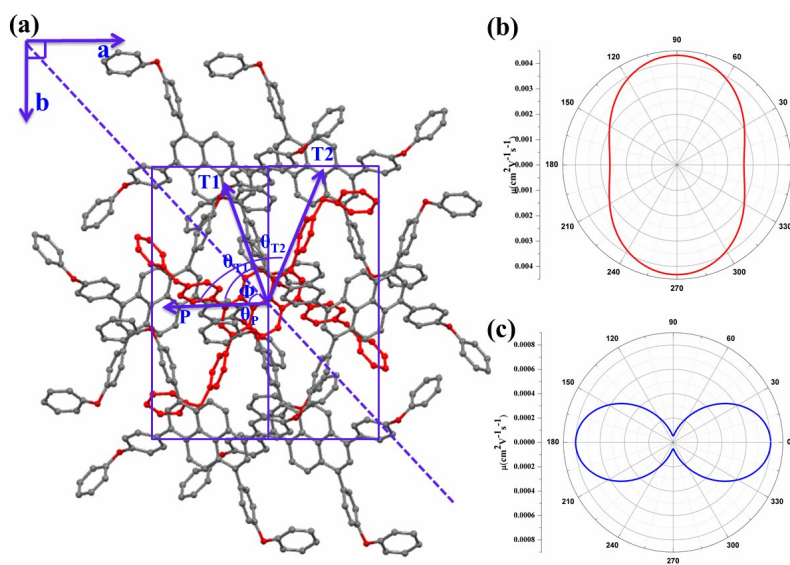


**Figure S11.** The projecting angle-dependent hopping paths to a transistor channel in the  $ab$  plane (a) and the calculated angle-resolved anisotropic hole (b) and electron (c) mobilities of molecule 2.



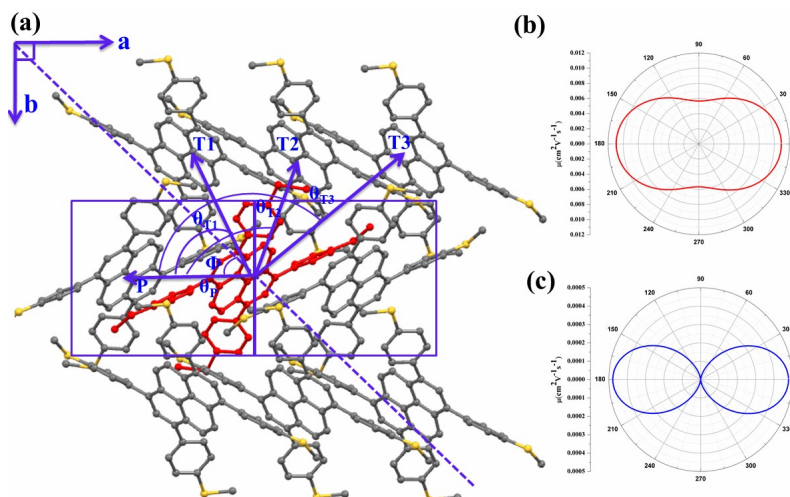


**Figure S12.** The projecting angle-dependent hopping paths to a transistor channel in the  $ab$  plane (a) and the calculated angle-resolved anisotropic hole (b) and electron (c) mobilities of molecule 3.

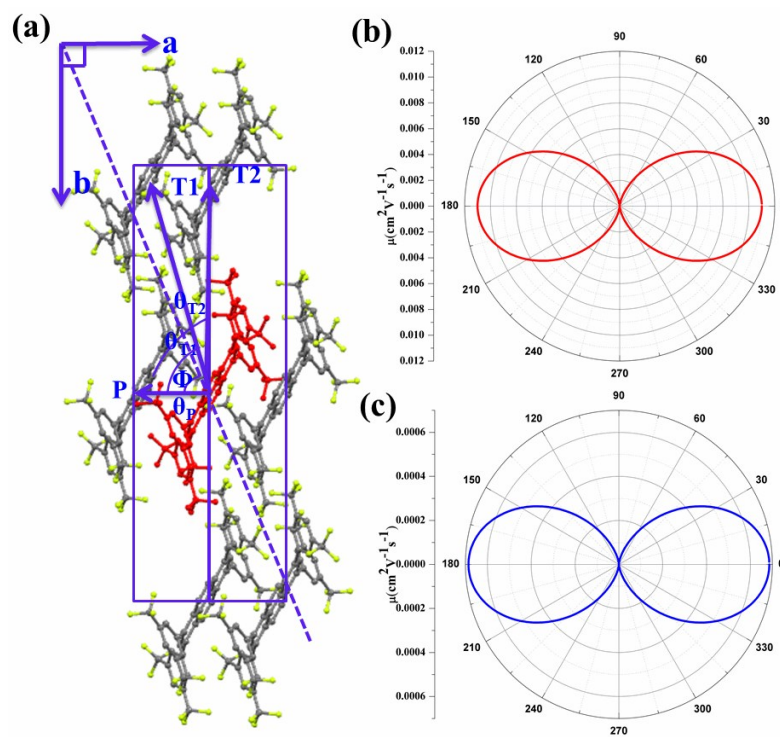


**Figure S13.** The projecting angle-dependent hopping paths to a transistor channel in the  $ab$  plane (a) and the calculated angle-resolved anisotropic hole (b) and electron (c) mobilities of molecule 5.

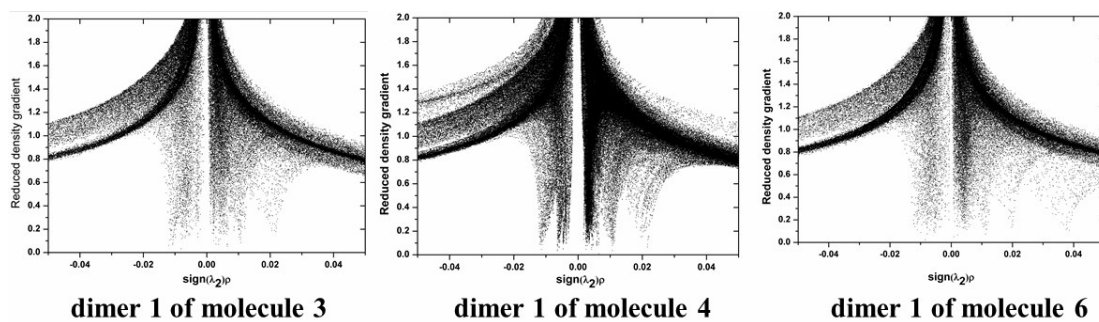


**Figure S14.** Plots of the reduced density gradient versus the electron density multiplied by the sign of the second Hessian eigenvalue. The data are obtained at B3LYP-D3/6-311G\* level.

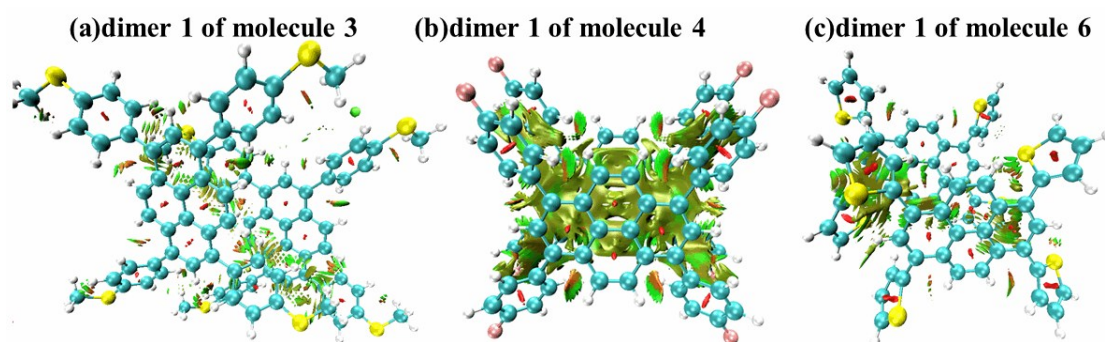


**Figure S15.** Gradient isosurfaces for (a) dimer1 of molecule 3, (b) dimer 1 of molecule 4, and (c) dimer 1 of molecule 6. The surfaces are colored on a blue-green-red scale according to values of  $\text{sign}(\lambda_2)\rho$ , ranging from -0.04 to 0.02 au. Blue indicates strong attractive interactions, green indicates Van der Waals interactions and red indicates strong repulsion.

**Table S1.** The selected optimized bond lengths, bond angles and dihedral angles of molecules 1 to 3 in the neutral and ionic states, together with experimental values<sup>1</sup> (the unit of bond lengths is in angstroms, and the bond angles and dihedral angles are in degrees).

Molecule	Bond Parameters	Neutral	Expt. <sup>1</sup>	Cationic	Anionic
1	R(C2-C3)	1.49	1.49	1.48	1.48
	R(C6-C7)	1.49	1.49	1.48	1.48
	R(C10-C11)	1.49	1.49	1.48	1.48
	R(C13-C14)	1.49	1.49	1.48	1.48
	$\theta$ (C2-C3-C4)	122.9	121.6	122.7	123.4
	$\theta$ (C6-C7-C8)	122.8	121.2	122.7	123.3
	$\theta$ (C9-C10-C11)	118.2	119.1	118.7	118.2
	$\theta$ (C9-C13-C14)	118.3	119.6	118.7	118.3
	$\theta$ (C1-C2-C3-C4)	53.5	53.6	48.5	45.1
	$\theta$ (C5-C6-C7-C8)	54.5	57.5	48.7	45.2
	$\theta$ (C9-C10-C11-C12)	50.2	51.5	44.7	41.9
$\theta$ (C9-C13-C14-C15)	51.1	55.5	44.9	42.1	
2	R(C2-C3)	1.49	1.48	1.47	1.48
	R(C6-C7)	1.49	1.48	1.47	1.48
	R(C10-C11)	1.49	1.48	1.47	1.48
	R(C13-C14)	1.49	1.48	1.47	1.48
	$\theta$ (C2-C3-C4)	122.8	123.5	122.7	123.2
	$\theta$ (C6-C7-C8)	122.8	122.4	122.8	123.3
	$\theta$ (C9-C10-C11)	118.3	118.0	118.8	118.3
	$\theta$ (C9-C13-C14)	118.3	118.4	118.7	118.2
	$\theta$ (C1-C2-C3-C4)	55.1	45.8	47.0	46.3
	$\theta$ (C5-C6-C7-C8)	55.8	65.9	47.0	45.8
	$\theta$ (C9-C10-C11-C12)	51.6	39.3	43.1	43.1
$\theta$ (C9-C13-C14-C15)	52.4	64.8	42.8	42.8	
3	R(C2-C3)	1.49	1.49	1.47	1.48
	R(C6-C7)	1.49	1.50	1.47	1.48
	R(C10-C11)	1.49	1.49	1.47	1.48
	R(C13-C14)	1.49	1.50	1.47	1.48
	$\theta$ (C2-C3-C4)	122.9	122.1	122.9	123.5
	$\theta$ (C6-C7-C8)	122.9	123.9	122.9	123.5
	$\theta$ (C9-C10-C11)	118.2	118.8	118.6	118.1
	$\theta$ (C9-C13-C14)	118.2	117.7	118.6	118.1
	$\theta$ (C1-C2-C3-C4)	54.9	52.2	47.1	44.4
	$\theta$ (C5-C6-C7-C8)	54.9	43.3	47.1	44.4
	$\theta$ (C9-C10-C11-C12)	51.3	49.9	42.9	41.7
$\theta$ (C9-C13-C14-C15)	51.3	38.2	42.9	41.7	

**Table S2.** The selected optimized bond lengths, bond angles and dihedral angles of molecules 4 to 6 in the neutral and ionic states, together with experimental values<sup>1</sup> (the unit of bond lengths is in angstroms, and the bond angles and dihedral angles are in degrees).

Molecule	Bond Parameters	Neutral	Expt. <sup>1</sup>	Cationic	Anionic
4	R(C2-C3)	1.49	1.49	1.48	1.48
	R(C6-C7)	1.49	1.50	1.48	1.48
	R(C10-C11)	1.49	1.49	1.48	1.48
	R(C13-C14)	1.49	1.50	1.48	1.48
	$\theta$ (C2-C3-C4)	122.8	122.6	122.7	123.2
	$\theta$ (C6-C7-C8)	122.8	123.3	122.7	123.2
	$\theta$ (C9-C10-C11)	118.3	119.0	118.7	118.3
	$\theta$ (C9-C13-C14)	118.3	118.0	118.7	118.3
	$\theta$ (C1-C2-C3-C4)	55.7	45.6	48.8	46.5
	$\theta$ (C5-C6-C7-C8)	55.8	45.2	49.0	46.5
	$\theta$ (C9-C10-C11-C12)	52.3	39.4	45.0	43.1
$\theta$ (C9-C13-C14-C15)	52.4	41.7	45.1	43.2	
5	R(C2-C3)	1.49	1.49	1.48	1.48
	R(C6-C7)	1.49	1.49	1.48	1.48
	R(C10-C11)	1.49	1.49	1.48	1.48
	R(C13-C14)	1.49	1.50	1.48	1.48
	$\theta$ (C2-C3-C4)	122.7	120.8	122.7	123.5
	$\theta$ (C6-C7-C8)	122.8	120.6	122.8	123.6
	$\theta$ (C9-C10-C11)	118.0	119.6	118.2	117.7
	$\theta$ (C9-C13-C14)	117.9	119.5	118.2	117.6
	$\theta$ (C1-C2-C3-C4)	59.0	51.8	52.6	46.5
	$\theta$ (C5-C6-C7-C8)	57.2	54.7	51.5	45.9
	$\theta$ (C9-C10-C11-C12)	57.2	54.1	51.2	46.2
$\theta$ (C9-C13-C14-C15)	55.3	51.4	50.2	45.6	
6	R(C2-C3)	1.47	1.48	1.46	1.46
	R(C6-C7)	1.48	1.49	1.46	1.46
	R(C10-C11)	1.47	1.48	1.46	1.46
	R(C13-C14)	1.48	1.49	1.46	1.46
	$\theta$ (C2-C3-C4)	122.3	121.3	122.1	122.7
	$\theta$ (C6-C7-C8)	123.7	122.7	124.0	124.4
	$\theta$ (C9-C10-C11)	118.8	119.1	119.4	118.8
	$\theta$ (C9-C13-C14)	117.3	117.6	117.4	117.0
	$\theta$ (C1-C2-C3-C4)	48.3	55.4	40.2	39.0
	$\theta$ (S5-C6-C7-C8)	55.3	60.5	42.6	45.5
	$\theta$ (C9-C10-C11-S12)	44.9	53.6	34.7	36.3
	$\theta$ (C9-C13-C14-C15)	47.5	55.9	35.0	36.9

**Table S3.** The transfer integrals of hole ( $V_{\text{hole}}$ ) and electron ( $V_{\text{electron}}$ ) (absolute value) for different hopping pathways of molecules 1 to 6 based on B3LYP/6-31G(d, p) level.

<b>Molecule</b>	<b>Pathway</b>	<b>Distance (<math>\text{\AA}</math>)</b>	<b><math>V_{\text{hole}}</math> (meV)</b>	<b><math>V_{\text{electron}}</math> (meV)</b>
1	1, 2, 3, 4	9.64	3.3	3.7
	5, 6, 7, 8	13.76	1.2	0.7
	9, 10, 11, 12	13.13	0.1	1.3
2	1, 2	7.20	18.6	9.4
	3, 4	14.61	$9.2 \times 10^{-4}$	$3.6 \times 10^{-4}$
	5, 6, 7, 8	10.47	8.2	3.0
	9, 10	19.36	0.04	0.04
	11, 12, 13, 14	16.46	0.09	0.02
3	1, 2	6.99	3.9	9.7
	3, 4, 5, 6	8.89	4.7	0.2
	7, 8	13.30	1.2	2.0
	9, 10, 11, 12	15.34	4.7	0.7
	13, 14	17.63	0.2	0.6
	15, 16	18.97	2.6	0.7
4	1, 2	3.91	18.7	27.9
	3, 4	12.56	0.2	0.3
	5, 6	12.56	$1.7 \times 10^{-3}$	0.01
	7, 8	11.93	1.3	0.1
	9, 10, 11, 12	15.31	0.3	0.2
	13, 14, 15, 16	15.26	0.2	0.06
5	1, 2	4.80	9.9	6.3
	3, 4	15.13	0.05	0.2
	5, 6	14.35	0.03	$3.9 \times 10^{-4}$
	7, 8, 9, 10	16.38	0.05	0.07
	11, 12, 13, 14	16.22	0.02	0.04
6	1, 2, 3, 4	6.93	18.2	3.0
	5, 6	10.99	5.9	3.5
	7, 8, 9, 10	13.38	0.3	2.0
	11, 12, 13, 14	17.08	$1.3 \times 10^{-3}$	$6.8 \times 10^{-4}$
	15, 16	13.98	2.2	2.8
	17, 18	13.69	5.8	4.1

**Table S4.** The calculated average mobilities of hole ( $\mu_{h,ave.}$ ) and electron ( $\mu_{e,ave.}$ ) of molecules 1 to 6 based on B3LYP/6-31G (d, p) level.

<b>Molecule</b>	<b><math>\mu_{h,ave.}</math> (cm<sup>2</sup>V<sup>-1</sup>s<sup>-1</sup>)</b>	<b><math>\mu_{e,ave.}</math> (cm<sup>2</sup>V<sup>-1</sup>s<sup>-1</sup>)</b>
1	$2.8 \times 10^{-3}$	$1.4 \times 10^{-3}$
2	$3.9 \times 10^{-3}$	$3.6 \times 10^{-4}$
3	0.01	$1.2 \times 10^{-4}$
4	0.01	0.01
5	$4.6 \times 10^{-3}$	$3.2 \times 10^{-4}$
6	0.02	$2.9 \times 10^{-3}$

**Table S5** Intermolecular interaction energies for the most prominent dimers of molecules 3, 4 and 6.

<b>Dimers</b>	<b>Interaction energies (kcal/mol)</b>
Dimer 1 of molecule 3	-31.75
Dimer 1 of molecule 4	-36.81
Dimer 1 of molecule 6	-24.74

**Table S6.** The reorganization energies of hole ( $\lambda^+$ ) and electron ( $\lambda^-$ ) using adiabatic potential energy surfaces (APES) approach, the HOMO, LUMO energies, as well as the vertical and adiabatic ionization potentials (IP<sub>V</sub>, IP<sub>A</sub>) and electron affinities (EA<sub>V</sub>, EA<sub>A</sub>) of molecule 6 at B3LYP-D3/6-31G (d, p) level: All the data are in unit of eV.

$\lambda^+$	$\lambda^-$	<b>HOMO</b>	<b>LUMO</b>	<b>IP<sub>V</sub></b>	<b>IP<sub>A</sub></b>	<b>EA<sub>V</sub></b>	<b>EA<sub>A</sub></b>
0.285	0.266	-5.05	-2.02	6.14	6.00	-0.89	-1.02



**Table S7** The transfer integrals of hole ( $V_{\text{hole}}$ ) and electron ( $V_{\text{electron}}$ ) (absolute value) for different hopping pathways and charge mobilities of hole and electron for molecule 6 based on B3LYP-D3/6-31G(d, p) level.

Molecule	Pathway	Distance (Å)	$V_{\text{hole}}$ (meV)	$V_{\text{electron}}$ (meV)
<b>6</b>	1, 2, 3, 4	6.93	18.4	3.0
	5, 6	10.99	6.0	3.5
	7, 8, 9, 10	13.38	0.3	2.0
	11, 12, 13, 14	17.08	$1.3 \times 10^{-3}$	$6.9 \times 10^{-4}$
	15, 16	13.98	2.2	2.9
	17, 18	13.69	5.9	4.2
$\mu$ ( $\text{cm}^2\text{V}^{-1}\text{s}^{-1}$ )			0.02	$3.2 \times 10^{-3}$

## References

1. T. H. El-Assaad, M. Auer, R. Castañeda, K. M. Hallal, F. M. Jradi, L. Mosca, R. S. Khnayzer, D. Patra, T. V. Timofeeva, J.-L. Brédas, E. J. W. List-Kratochvil, B. Wex, and B. R. Kaafarani, *J. Mater. Chem. C*, 2016, **4**, 3041–3058.